Fluorescence profiles and cooling dynamics of laser-cooled Mg^+ ions in a linear rf ion trap

XianZhen Zhao,* Vladimir L. Ryjkov,† and Hans A. Schuessler
Department of Physics, Texas A&M University, College Station, Texas 77843, USA
(Received 26 July 2005; revised manuscript received 9 January 2006; published 9 March 2006)

Fluorescence line profiles and their implications on the cooling dynamics of the Mg^+ ions stored in a linear rf trap are studied. The line profile is dictated by the temperature of the ion cloud at different laser detunings. The upper bound of the lowest temperature was estimated for different values of the rf trapping potential amplitude and the buffer gas pressure. A general trend of this ultimate temperature to increase with the rf trapping voltage and buffer gas pressure is expected, with an abrupt change at some critical value corresponding to the transition to and from a strongly correlated liquid or crystal state. While on the one hand this expectation was confirmed when the buffer gas pressure was varied; on the other hand the influence of the amplitude of the trapping voltage on the ultimate temperature shows an interesting new feature of first dipping down before the sharp increase occurs.

DOI: 10.1103/PhysRevA.73.033412 PACS number(s): 32.80.Pj, 32.70.Jz, 42.50.Vk

I. INTRODUCTION

Rf ion traps [1] are excellent devices for high precision measurements due to their ability to confine ions for long periods of time in an isolated high-vacuum environment. When laser cooling [2] is applied to trapped ions, their temperature can be reduced to the milliKelvin range, therefore, drastically improving the conditions for precision optical measurements. The benefits of laser cooling can even be extended to those ions that cannot be directly laser-cooled. This is achieved through sympathetic cooling [3–5], when the ions of interest are added to the ion clouds which can be directly laser-cooled; through Coulomb interaction the added ions are also cooled down.

There are several factors that affect the temperature of the laser-cooled ions. First, the efficiency of laser cooling depends on the temperature and the laser detuning. This process is well understood and accurately described [2]. Second, there is the rf heating effect, which increases the temperature of the ion cloud. It depends on the temperature, the trapping voltage, and the size of the ion cloud. To optimize laser cooling and sympathetic cooling it is essential to have a good understanding of all heating processes that occur in the stored ion cloud.

The very early laser cooling experiments on a few ions in rf ion traps [6] have shown effects similar to a phase transition at low temperatures. Some aspects of this behavior have been successfully described in the framework of order-chaos transition [7,8] in this nonlinear mechanical system. However, recent laser cooling experiments involve larger and larger ion crystals [9,10]. As more ions are introduced into the trap, the few body dynamics description should be replaced by a statistical approach. The initial effort to create a statistical model of the rf heating process can be traced to the early days of laser cooling [11]. This approach, modified and refined [12,13] since, treats rf heating as a result of two-body Coulomb collisions, and finds the rf heating rates by evaluating pair collision integrals. The result is in qualitative agreement with the experiment, as the predicted rf heating rate has a maximum at some low temperature and decreases at both higher and lower temperatures. However, it is debatable if the pair collision approach can be used at the ultralow temperatures (e.g., below a few kelvins), since in this region the ion correlation effects are stronger. Another route to investigate the properties of rf heating is to use computer simulations to calculate rf heating rates by simulating the motion of ions in the trap. This approach has also been initiated early [14], and has identified some of the important features of the rf heating effect. More recent results [15–18] show some very interesting properties of the rf heating effect.

While the theoretical and experimental investigations [6–17] into properties of rf heating explore different regimes, they are all in agreement on one important aspect: when the temperature of the ion cloud is brought below a certain level, the heating rate starts to decrease with temperature. As a consequence, below that temperature the rf heating will *not* prevent further cooling of the ion cloud. The minimum temperature will then be established by the equilibrium of the laser cooling by a heating process other than rf heating (ion-ion interactions in the rf field). One such limit is due to the photon recoil heating. Also, in the miniature rf traps that are being utilized as one of the quantum computing implementations, surface effects start to play a role in the heating of the ions [19–21]. However, the surface and photon recoil heating effects are small (i.e., result in the equilibrium temperature on the order of a few milliKelvin), and cannot account for the effects reported in this paper. In this article, we present our investigations of the low temperature limits achieved by ion clouds under different trapping conditions.

II. EXPERIMENTAL METHODS

The trap used in our experimental investigation is described in more detail elsewhere [22]. Here we summarize the parameters briefly. The trap consists of four identical cy-

*Presently at Department of Chemistry, University of British Columbia, Vancouver, British Columbia, Canada.
†Presently at TRIUMF, Vancouver, British Columbia, Canada.

lindrical electrodes. Each of the four electrodes has a diameter of 6 mm and is broken into three 50 mm long segments for more flexible dc voltage applications. The rf voltages are applied to the two pairs of connected opposing electrodes, which creates an oscillating quadrupole potential in the radial direction,

$$\phi(x,y;t) = (U - V\cos(\Omega t))\frac{x^2 - y^2}{r_0^2}, \quad (1)$$

where $-V\cos(\Omega t)$ is the applied rf signal, U is the quadrupole dc offset ($U=0$ in our experiments), and r_0 is the distance from the trap axis to the electrode surface. The motion of a single ion in this potential is described by the Mathieu equations [23] with characteristic parameters $q = 4eV/mr_0^2\Omega^2$, $a=0$. Along the trap axis the ions are confined by the dc bias voltages applied to each of the three trap segments. Mg^+ ions used in the measurements are generated by electron bombardment of their thermal neutral atomic beam.

The $3s\ ^2S_{1/2} \rightarrow 3p\ ^2P_{3/2}$ optical transition of Mg^+ ions is used. An UV laser beam with a wavelength of about 280 nm is required for laser cooling of the Mg^+ ions at this optical transition. It is obtained by frequency doubling a cw dye laser (Coherent 699-21) in an external cavity. The UV beam is directed along the trap axis as illustrated in Fig. 1. The laser induced fluorescence signal is detected by a photomultiplier tube (PMT) located at one side of the trap. The number of ions inside the trap can be measured by ejecting the ions onto a secondary electron multiplier (SEM) located on the opposite side of the trap. All measurements reported here were performed following the same procedure for loading the ions into the trap to ensure that the number of ions is kept the same (about 10^4) for every measurement.

III. STATISTICAL APPROACH TO ION CLOUDS STORED IN A RF FIELD

The temperature of the ions stored in the ion trap is determined by three coexisting processes that either increase (heat) or decrease (cool) the kinetic energy of the trapped ions:

(1) laser cooling or heating;
(2) rf heating;
(3) buffer gas (helium in our experiments) cooling/heating.

At equilibrium the net flow of kinetic energy is zero, i.e.,

$$\frac{dQ_L}{dt} + \frac{dQ_{RF}}{dt} + \frac{dQ_B}{dt} = 0. \quad (2)$$

This equation determines the equilibrium temperature of the system. At a fixed laser detuning, given enough time, the ion cloud will reach an equilibrium temperature which satisfies Eq. (2). If the quantitative descriptions of the three contributions were all available, then Eq. (2) could be used to predict the ion cloud temperature for any arbitrary laser detuning, and, therefore, the line shape of the fluorescence signal.

However, out of the three processes that determine the temperature of the ion cloud, only the interaction with the laser radiation has an accurate analytical description [2]

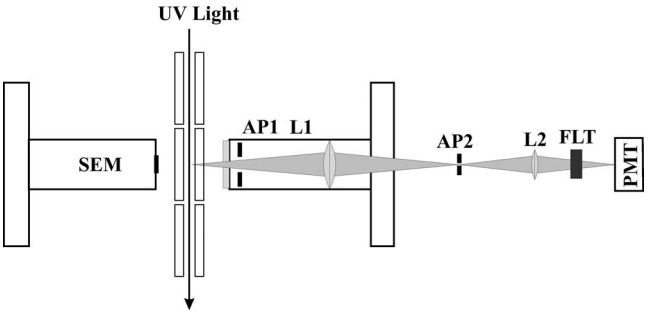

FIG. 1. Schematics of the ion trap together with the detection systems.

$$\frac{dQ_L}{dt} = C\,\mathrm{Re}[(\Delta + \alpha\Gamma + i\Gamma)w(\Delta + i\Gamma)], \quad (3)$$

where $\Gamma = \gamma(c/\omega)\sqrt{m/2k_BT}$ characterizes the Doppler linewidth of the transition at the given temperature T; $\Delta = (\omega_0 - \omega)(c/\omega)\sqrt{m/2k_BT}$ characterizes the transition of the laser frequency ω from the atomic transition frequency ω_0; $\alpha = \hbar\omega^2/mc^2\gamma$ is the characteristic value of the transition's recoil energy. The function $w(\Delta + i\Gamma)$ is known as the Faddeeva function or the plasma dispersion function. k_B is the Boltzmann constant. The constant C collects all the proportional factors, such as the total number of ions, the laser intensity, the radiation rate, etc.

The theoretical models based on the ion-ion Coulomb collision rates [11,13] capture the general characteristics of the rf heating, mainly the fact that it decreases both at high and low temperatures. Such models are expected to work better at higher temperatures, where the potential energy of the Coulomb interaction is much less than the kinetic energy of the ions. Application of the binary collision picture at low temperatures cannot be strictly justified. However, it has descriptive value in the absence of more accurate low temperature models. Currently, computer simulations [15–17] provide the most accurate information about the properties of the rf heating, and have helped to identify some of its interesting properties at low temperatures. However, at this time there are no theoretical models that describe the features of the rf heating that are in the focus of this research. It is also important to note that the binary collision model mentioned above has been used successfully for describing the fluorescence line profiles in an rf Paul trap of traditional geometry [24] (consisting of a ring and two cap electrodes). In that case the rf heating rate was quite high and the ions did not reach temperatures below 10 K, so the binary collision model could be used.

A simple statistical model of the energy exchange between the ion cloud and the buffer gas through collisions suggests the following expression for the rate:

$$\frac{dQ_B}{dt} = B(T_B - T), \quad (4)$$

where T_B is the buffer gas temperature (room temperature in our experiments). Coefficient B can be calculated from the

collision cross section between the ions and the helium atoms. This model ignores the fact that the ions are subject to the rf trapping field. A more accurate description of this effect will be obtained when the motion of the ion cloud in the rf field is better understood.

IV. RESULTS AND DISCUSSION

In our experiments the UV beam frequency is initially set to a frequency several GHz below the cooling transition. It is then swept at a constant rate across the transition while the fluorescence from the trapped Mg^+ ions is recorded. The fluorescence line shape produced in such an experiment is found to be of two major types.

Figure 3(c) is an example of the first type, where the ion cloud goes through a "phase transition," when the temperature of the cloud sharply decreases. This temperature decrease is often exhibited by a sudden drop in the fluorescence signal at a large red detuned frequency. It is due to the form of the dependence of the rf heating rate on the temperature of the ion cloud, namely the fact that it reaches maximum at some low temperature (typically around few degrees Kelvin) and decreases both towards high and low temperatures. If the laser cooling rate is high enough to overcome the critical point where the heating is maximum, the cloud temperature drops sharply. It should be noted that this temperature drop does not necessarily result in a formation of an ion crystal [10]. As the laser frequency continues to get closer to the transition, the fluorescence increases, then again drops at the transition frequency. This second sharp drop in the fluorescence rate is, however, due to a sharp decline in cooling efficiency when the laser frequency gets close to the cooling transition [2]. Consequently, the ion cloud quickly heats up. Above the transition frequency, laser cooling turns into laser heating. As a result, the temperature of the ion cloud is high, and the fluorescence signal is low. The resulting fluorescence line shape is a combination of two asymmetric peaks, a wide and low peak at a large detuning succeeded by a narrow and high peak close to the transition frequency. One of the examples of the second type is shown in Fig. 3(a), where the laser cooling efficiency is not high enough to overcome the heating processes that affect the ion cloud. Therefore the temperature is significantly higher than in the first case, and the narrow high peak corresponding to ultralow temperature is not observed. At higher temperatures the cooling efficiency decreases more slowly around the cooling transition, which results in a slower decrease in the fluorescence around the transition frequency.

While more detailed understanding is needed for the exact interpretation of the cooling fluorescence line shapes, we still can use them to make an upper bound estimate of the lowest achieved temperature. The following properties of the fluorescence line shape allow for this estimate. First, the decrease in the fluorescence when the laser frequency is close to the cooling transition is an accurate indicator of the resonance frequency. It has been verified with the Doppler-free saturation spectroscopy of iodine hyperfine lines. It is more accurate for the curves with ultralow temperature narrow peaks due to the fact that rf heating is greatly reduced at these temperatures, and the fluorescence decrease is very steep. Second, at any given temperature, laser cooling is the most efficient around the half-width of the fluorescence line shape [2]. To make the upper bound estimate, we first determine the difference between the frequency at which the fluorescence reaches half of the maximum value and the frequency at which it is decreased to 10% of the maximum. This difference corresponds to half of the linewidth of the fluorescence at the temperature to be estimated; and then the temperature can be obtained using the Voigt line profiles for this linewidth.

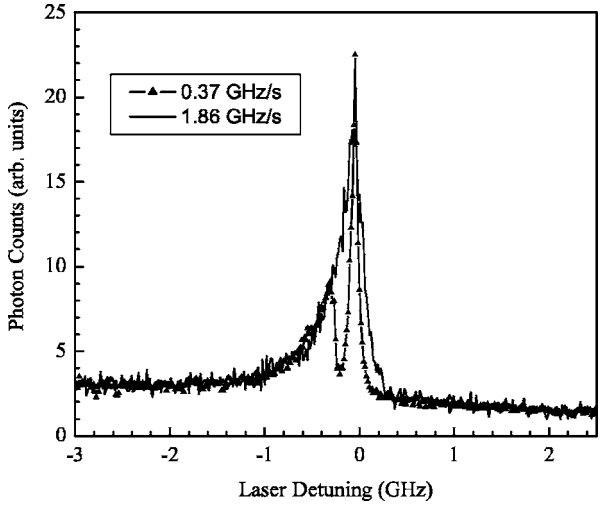

FIG. 2. LIF of Mg^+ for different UV scanning speeds. The UV power is 140 μW. The number of ions is about 10^4. The rf voltage is 235 V, peak to peak.

One of the important issues in the interpretation of the fluorescence is whether the ion cloud is in equilibrium at every step of the laser scan. This is particularly important at the areas of the scan where the temperature of the ion cloud changes significantly over a narrow interval of laser frequency. This aspect was studied by comparing the fluorescence line shapes obtained with different UV laser scan speeds, two such examples are illustrated in Fig. 2.

From the figure it is clear that for the UV scanning speed of 1.86 GHz/s, there is only one asymmetric peak, whereas at the speed of 0.37 GHz/s, there are two peaks. This shows that in the first case, the ion cloud fails to reach the ultralow temperatures, while in the second case it does achieve the ultralow state during the laser scan. It is also found that when the UV scanning speed is slower than 0.37 GHz/s the fluorescence line shape of the cooling process remains the same. This means that the ion ensemble during the entire scan is in thermal equilibrium state for every frequency detuning. Based on the scan speed and our temperature data we estimate that it takes a few 100 ms for the ion cloud to drop from 20 to 30 K to below 0.1 K.

Fig. 3 shows the fluorescence line shapes at different rf trapping voltages. At higher temperatures where the ion cloud has not formed an organized crystal structure, our molecular dynamics simulations have shown that rf heating is proportional to the fourth power of rf voltage [17]. If this trend is reproduced at ultralow temperatures as well, then the

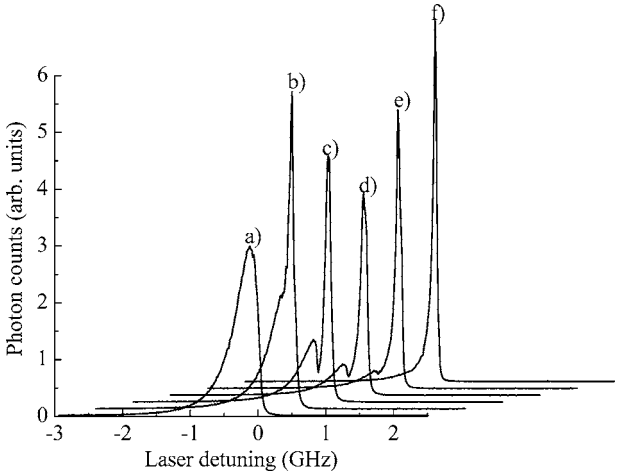

FIG. 3. Effect of rf voltages on the LIF line shape of Mg^+ ions. The UV scanning speed is 92.8 MHz/s. The UV beam power is kept around 120 μW. There are about 10^4 ions in the trap. The rf trapping voltages (peak to peak values) are (a) 570 V, (b) 467 V, (c) 395 V, (d) 318 V, (e) 241 V, and (f) 166 V, respectively. All the graphs are plotted in the same scale. Each graph is shifted horizontally and vertically relative to the previous one for better viewing and comparison purposes.

linewidth, and the corresponding minimum temperature, would steadily increase with the trapping voltage. However, the experimental results show some very interesting, new effects, as seen in Fig. 4. Indeed as the rf voltage is increased, initially the linewidth increases as well. Yet, after the trapping voltage exceeds 318 V, peak to peak, the linewidth begins to decrease. Then, at yet higher trapping voltages when the laser cooling strength becomes insufficient to cool the cloud into the organized ultra-low temperature state, the linewidth experiences a large jump. The linewidth is also indirectly revealed by the height of the fluorescence peak as seen from Fig. 3.

It is important to stress that the existing physical picture of the rf heating predicts the ultimate temperature is limited by factors other than rf heating due to ion-ion interaction.

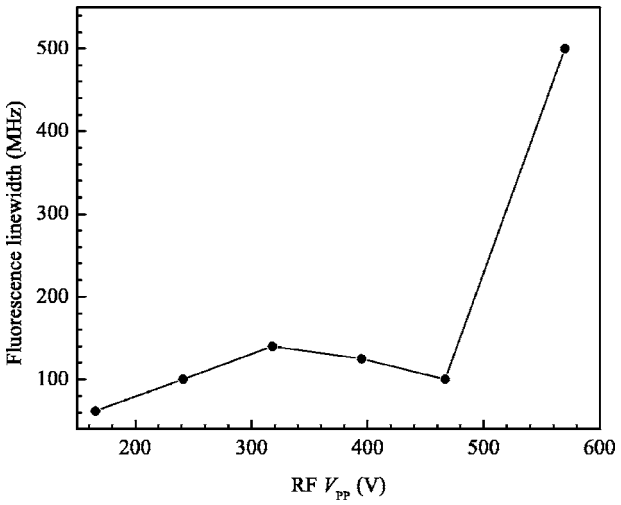

FIG. 4. Change of the fluorescence linewidth as a function of the trapping voltage.

None of the presently known factors can explain the behavior reported here, particularly the change in dependence on the rf amplitude. In our opinion the unexpected behavior is due to the stronger ion-ion correlation in an ion cloud at the higher trapping voltages. The results of our MD simulations [17] suggest that some ion clouds are more "stable" than others, depending on the underlying shell structure. The rf dependence reported here could be explained by the transition from a less to a more stable ion cloud, as the ion density changes with the rf field.

It should also be pointed out that our results are partially supported by the observations of ion cloud imaging while it is laser cooled. In Ref. [10] it is reported that the ion cloud initially condenses into a liquidlike state at the point of the fluorescence dip and then crystallizes as the laser detuning is further changed, and the laser cooling strength is increased. This is in contrast to the present picture of the rf heating that predicts the ion cloud to immediately reach the Doppler-limited temperature and thus the crystalline state. Further theoretical and experimental effort is required to exactly understand the processes involved in dynamics of laser cooling of rf confined ion clouds.

Another indicator of the rf heating properties is the position of the first fluorescence dip that separates the wide and narrow portions of the double peak fluorescence line shape. This dip occurs when the laser cooling overpowers the combination of the rf and buffer gas heating and cools the cloud into the ultralow temperature state. From Fig. 3 one can observe that the position of this dip is steadily moved closer to the transition frequency when the rf voltage is increased. This behavior is due to the increase in the rf heating with the trapping voltage.

The influence of the buffer gas pressure on the achievable fluorescence linewidth, and thus the ion cloud temperature is also investigated and illustrated in Fig. 5. In our experiments the laser cooling strength was sufficient to bring the ions to the temperatures well below room temperature. Therefore the influence of the buffer gas collisions is only that of heating when laser cooling is in effect. When no helium buffer gas is introduced, the background pressure is very low ($<10^{-9}$ mbar), which means that the average time interval between collisions between the buffer gas and the ion cloud is on the order of several minutes per ion. In this practically collision-free environment the phase transition from the unordered ion cloud to the ordered ion crystal structure is clearly observed as a characteristic dip. As the buffer gas pressure is increased, the fluorescence signal peak becomes shorter and wider, indicating that the temperature of the ion cloud is increasing. Therefore for a given UV power (thus certain laser cooling capability), the buffer gas is heating up the ion cloud, in agreement with the equation of energy balance Eq. (2).

The forementioned method of making an upper bound estimate of the minimum attained temperature is again used for each of the pressures in Fig. 5. Then the change of the ion temperature versus buffer gas pressure is plotted in Fig. 6. The heat exchange between the buffer gas and the trapped ions should be proportional to the number density of the buffer gas atoms, and therefore the buffer gas pressure. We expect a general increasing trend of the temperature of the

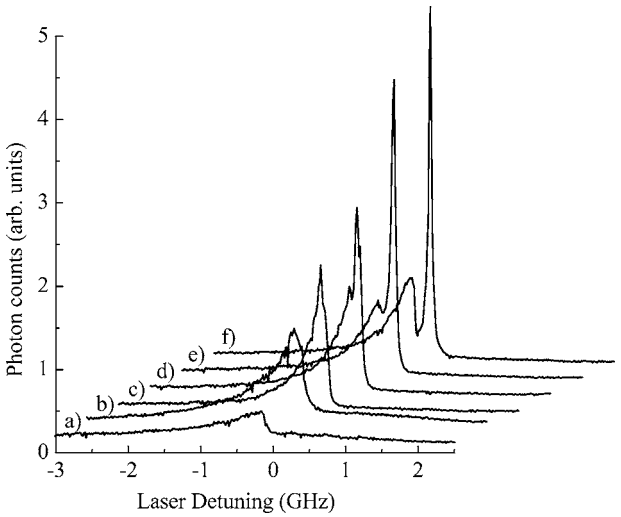

FIG. 5. LIF signal of Mg^+ for different buffer gas pressures. The UV beam frequency is scanned at a speed of 92.8 MHz/s. The rf voltage is 216 V, peak to peak. There are about 10^4 ions in the trap. The UV beam power is kept at 115 μW. The helium buffer gas pressures are (a) 2×10^{-6} mbar, (b) 1×10^{-6} mbar, (c) 1.6×10^{-7} mbar, (d) 7×10^{-8} mbar, (e) 4×10^{-8} mbar, and (f) no added buffer gas, with a background pressure $<1\times10^{-9}$ mbar, respectively. All the graphs are plotted in the same scale. Each graph is shifted horizontally and vertically relative to the previous one for better viewing and comparison purposes.

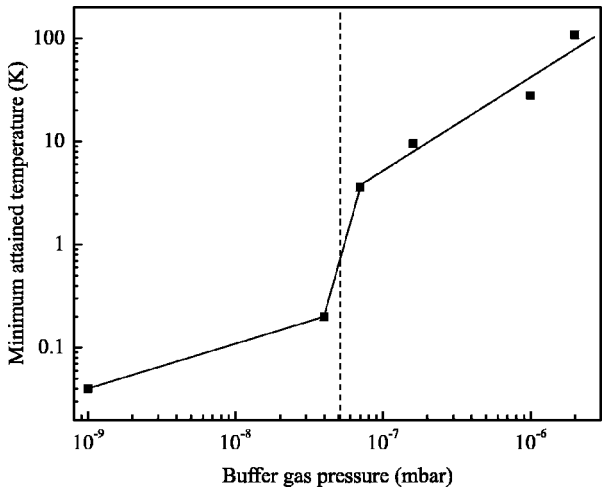

FIG. 6. Change of the minimum attained temperature as a function of the buffer gas pressure. Both the solid and dashed lines are merely visual guides.

ion cloud as the buffer gas pressure increases. The experimental data agrees with this prediction in general. For the pressures above 7×10^{-8} mbar the dependence appears to be linear. For the pressures below 4×10^{-8} mbar, it again reduces slowly. Of particular importance is the sudden increase in the ion temperature when the buffer gas pressure is changed from 4×10^{-8} to 7×10^{-8} mbar. This is a consequence of the given laser cooling power not being able to overcome the combination of the rf and buffer gas heating. Therefore in our experiments after this pressure, the laser cooling power is no longer sufficient to maintain the ions in the ultralow temperature state; as a result the temperature goes up drastically.

V. SUMMARY

We have presented our studies of the changes in the fluorescence line shape as we change the parameters of three competing processes: laser cooling, rf heating, and buffer gas heating. The line shapes were used to obtain an upper bound estimate of the lowest temperature reached by the ion cloud. Two main classes of the fluorescence line shapes were observed: the broad asymmetric single peak shape characteristic of higher ($T>10$ K) temperatures, and the double peak with a very narrow line corresponding to the ion cloud at the sub-Kelvin temperatures. Variations of the buffer gas pressure have produced the expected result of the lowest temperature increasing with an increase in buffer gas pressure. We have also observed an abrupt jump in temperature corresponding to the critical heating rate that must be overcome for the transition of the ion cloud into strongly-correlated low temperature liquid or crystal state to occur. Variation of the rf trapping voltage has revealed a new phenomenon. While all of the existing theories predict the general trend of the rf heating to increase with the trapping voltage, we have observed that the ion cloud temperature initially increases, but then shows a decrease as the trapping voltage is increased. With a further increase of the trapping voltage the temperature increases again, and also shows the abrupt jump corresponding to the critical heating rate. We have also estimated the thermalization time of the ion cloud in this laser cooling process to be several hundred milliseconds.

ACKNOWLEDGMENTS

We gratefully acknowledge the financial support from the Welch foundation under Grant No. A-1546.

[1] P. K. Ghosh, *Ion Traps* (Clarendon, Oxford, 1995), and references therein.

[2] D. J. Wineland and W. M. Itano, Phys. Rev. A **20**, 1521 (1979).

[3] P. Bowe, L. Hornekaer, C. Brodersen, M. Drewsen, J. S. Hangst, and J. P. Schiffer, Phys. Rev. Lett. **82**, 2071 (1999).

[4] K. Molhave and M. Drewsen, Phys. Rev. A **62**, 011401 (2000).

[5] B. B. Blinov, L. Deslauriers, P. Lee, M. J. Madsen, R. Miller, and C. Monroe, Phys. Rev. A **65**, 040304(R) (2002).

[6] F. Diedrich, E. Peik, J. M. Chen, W. Quint, and H. Walther, Phys. Rev. Lett. **59**, 2931 (1987).

[7] J. Hoffnagle, R. G. DeVoe, L. Reyna, and R. G. Brewer, Phys. Rev. Lett. **61**, 255 (1988).
[8] R. Blumel, C. Kappler, W. Quint, and H. Walther, Phys. Rev. A **40**, 808 (1989).
[9] M. Drewsen, C. Brodersen, L. Hornekær, J. S. Hangst, and J. P. Schiffer, Phys. Rev. Lett. **81**, 2878 (1998).
[10] L. Hornekær and M. Drewsen, Phys. Rev. A **66**, 013412 (2002).
[11] Y. Moriwaki, M. Tachikawa, Y. Maeno, and T. Shimizu, Jpn. J. Appl. Phys., Part 1 **31**, L1640 (1992).
[12] Y. Oshima, Y. Moriwaki, and T. Shimizu, Prog. Cryst. Growth Charact. Mater. **33**, 405 (1996).
[13] T. Baba and I. Waki, Appl. Phys. B: Lasers Opt. **74**, 375 (2002).
[14] J. D. Prestage, A. Williams, L. Maleki, M. J. Djomehri, and E. Harabetian, Phys. Rev. Lett. **66**, 2964 (1991).
[15] J. Wei, H. Okamoto, and A. M. Sessler, Phys. Rev. Lett. **80**, 2606 (1998).
[16] J. P. Schiffer, M. Drewsen, J. S. Hangst, and L. Hornekær, Proc. Natl. Acad. Sci. U.S.A. **97**, 10697 (2000).
[17] V. L. Ryjkov, X. Z. Zhao, and H. A. Schuessler, Phys. Rev. A **71**, 033414 (2005).
[18] S. Schiller and C. Lämmerzahl, Phys. Rev. A **68**, 053406 (2003).
[19] Q. A. Turchette, D. Kielpinski, B. E. King, D. Leibfried, D. M. Meekhof, C. J. Myatt, M. A. Rowe, C. A. Sackett, C. S. Wood, W. M. Itano, C. Monroe, and D. J. Wineland, Phys. Rev. A **61**, 063418 (2000).
[20] R. G. DeVoe and C. Kurtsiefer, Phys. Rev. A **65**, 063407 (2002).
[21] L. Deslauriers, P. C. Haljan, P. J. Lee, K.-A. Brickman, B. B. Blinov, M. J. Madsen, and C. Monroe, Phys. Rev. A **70**, 043408(R) (2004).
[22] X. Zhao, V. L. Ryjkov, and H. A. Schuessler, Phys. Rev. A **66**, 063414 (2002).
[23] N. W. McLachlan, *Theory and Application of Mathieu Functions* (Dover, New York, 1964).
[24] Y. Maeno, M. Tachikawa, Y. Moriwaki, and T. Shimizu, Jpn. J. Appl. Phys., Part 1 **34**, L174 (1995).